Journal Name

ARTICLE TYPE

Isoreticular metal-organic frameworks based on a rhombic dodecahedral metal-organic polyhedron as a tertiary building unit†

Dongwook Kim,[a] Xinfang Liu,[a] Minhak Oh,[a] Xiaokai Song,[ab] Yang Zou,[c]* Devendra Singh,[ad] Kwang S. Kim[ad] and Myoung Soo Lah[a]*

The solvothermal reactions of a Zn(II) ion with ligands containing two 1,3-benzene dicarboxylate residues linked via bent organic linkers with different flexibilities resulted in the isoreticular metal–organic frameworks (MOFs), PMOF-4 and PMOF-5, based on a rhombic dodecahedral metal–organic [10] polyhedron (MOP) as a tertiary building unit (TBU). The rhombic dodecahedral MOP was built using six $[Zn_2(COO)_4]$ clusters as a 4-c secondary building unit (SBU) and eight $[Zn_2(COO)_3]$ clusters as a 3-c SBU. The network of the isoreticular MOFs based on the rhombic dodecahedral Zn-MOP was a 3,3,4-c net with a **zjz** topology, which was different from those of the similar MOFs, PMOF-3 and PCN-12, based on a cuboctahedral Cu-MOP as a 24-c TBU. However, both 24-c TBUs in all MOFs were [15] quadruply interlinked to six neighboring TBUs to form the same **pcu** underlying topology.

Introduction

The prediction of the structure and topology of a new metal–organic framework (MOF) is an extremely difficult task.[1] Even a small change in the reactants and/or in the reaction conditions, [20] such as solvents, concentrations of the reactants, temperature, pH values, and counter ions, may lead to a completely different framework structure. The main reason for this problem stems from the difficulty in predicting the structure of a metal node as a primary building unit (PBU), or of a metal cluster node as a [25] secondary building unit (SBU). It is well known that a Cu(II) ion with a ligand containing a carboxylate residue has a strong preference for square-paddle-wheel $[Cu_2(COO)_4]$ SBUs.[2] The reaction of a Cu(II) ion with 1,3,5-benzenetricarboxylate (BTC) in various solvents led to HKUST-1(Cu) ($[Cu(II)_3(BTC)_2S_3]$, in [30] which S is the ligated solvent molecule), with a 3,4-c **tbo** topology.[3] In the network, the BTC ligand serves as a 3-c organic node with $3m$ point symmetry, and the $[Cu_2(COO)_4]$ serves as a 4-c metal cluster SBU with mmm point symmetry.[4] The reaction of a Cu(II) ion with 1,3-benzenedicarboxylate (1,3-BDC) also [35] generated either the 2-D MOF $[Cu(II)(1,3\text{-}BDC)S_2]$ (in which S is the ligated solvent molecule),[5] with a 4-c **sql** topology, or a cuboctahedral metal–organic polyhedron (MOP), $[Cu_{24}(1,3\text{-}BDC)_{24}S_{24}]$;[6] both were based on the same $[Cu_2(COO)_4]$ as a 4-c metal cluster SBU. However, a Zn(II) ion with a ligand [40] containing a carboxylate residue does not have as strong a preference for a square-paddle-wheel $[Zn_2(COO)_4]$ SBU as does a Cu(II) ion. Depending on reaction conditions, not only mononuclear Zn(II) centers of diverse coordination environments, such as PBUs,[7] but also various other metal clusters, such as [45] $[Zn_4O(COO)_6]$,[8] $[Zn_3(COO)_6]$,[9] $[Zn_2(COO)_4]$,[10] and $[Zn_2(COO)_3]$,[11] have been reported as SBUs. Although the

solvothermal reaction of a Zn(II) ion with BTC in DMF resulted in the isostructural HKUST-1(Zn) $[Zn(II)_3(BTC)_2S_3]$ with the same 3,4-c **tbo** topology based on the dinuclear metal cluster [50] $[Zn_2(COO)_4]$ as a 4-c SBU,[12] similar reactions in different solvents and/or in the presence of a template, such as serine, produced the MOF $[Zn_2(BTC)_2(NO_3)S_3]$, with a different net topology: a regular **srs** topology,[13] in which both the ligand and the other dinuclear metal cluster, $[Zn_2(COO)_3]$, served as a 3-c [55] SBU with a 32-point symmetry.[14]

The reaction of a Zn(II) ion with 1,3-BDC also produces a 2-D MOF based on the $[Zn_2(COO)_4]$ metal cluster as a 4-c SBU.[5] Although there are several reports of the preparation of the cuboctahedral Cu-MOP, $[Cu_{24}(L)_{24}S_{24}]$, based on the [60] $[Cu_2(COO)_4]$ SBU using either 1,3-BDC or its derivatives as a bent ditopic linker ligand (L) between the $[Cu_2(COO)_4]$ SBUs,[15] the corresponding isostructural cuboctahedral Zn-MOP, $[Zn_{24}(L)_{24}S_{24}]$, based on the 4-c $[Zn_2(COO)_4]$ SBU has not been reported. In addition, several MOFs based on the cuboctahedral [65] Cu-MOP as a supramolecular tertiary building unit (TBU) have been reported by using ligands containing two or three covalently linked 1,3-BDC residues,[16] whereas only a few corresponding MOFs based on a cuboctahedral Zn-MOP are known,[17] which is probably related to the limited stability of the $[Zn_2(COO)_4]$ SBU.

[70] In this study, we report two isoreticular polyhedron-based MOFs (PMOFs) that were obtained by using two tetracarboxylate ligands containing two 1,3-BDC residues linked via two long covalent linkers with different flexibilities (Scheme 1). We also investigated the structural and topological characteristics of the [75] PMOFs.

5,5'-(1,3-phenylenedi-2,1-ethynediyl)
bis(1,3-benzenedicarboxylic acid) (H₄L**1**)

5,5 -[1,3-phenylenebis(carbonylimino)]
bis(1,3-benzenedicarboxylic acid) (H₄L**2**)
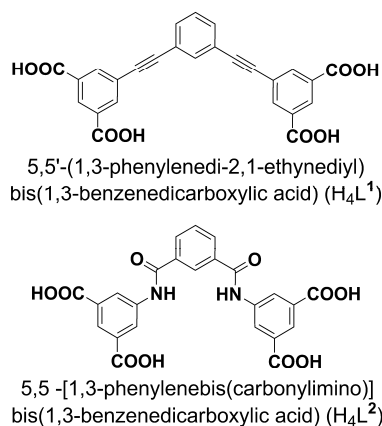
Scheme 1. Two tetracarboxylate ligands containing two 1,3-BDC residues.

Experimental section

General procedures. All reagents were purchased from commercial sources and used without further purification. Elemental analyses (C, H, and N) were performed at the Central Research Facilities of the Ulsan National Institute of Science & Technology. FT-IR spectra were recorded as KBr pellets on a Nicolet iS IO FT-IR spectrophotometer using the reflectance technique (4000–400 cm⁻¹). Thermal gravimetric analysis (TGA) data were recorded on a TA Instruments Q-600 series thermal gravimetric analyzer in a nitrogen atmosphere. Powder X-ray diffraction (PXRD) data were recorded using a Rigaku D/M 2200T automated diffractometer at room temperature, with a step size of 0.02° in a 2θ angle. Simulated PXRD patterns were calculated with the Material Studio program[18] using the single crystal data. 5,5′-(1,3-phenylenedi-2,1-ethynediyl)bis(1,3-benzenedicarboxylic acid) (H₄L**1**) was prepared according to the reported procedure.[14b]

Preparation of 5,5′-[1,3-phenylenebis(carbonylimino)]bis(1,3-benzenedicarboxylic acid) (H₄L²). 1,3-Benzenedicarboxylic acid chloride (3.04 g; 14.97 mmol) was added to a solution of 8.16 g (45.05 mmol) of 5-amino isophthalic acid and 3.60 mL (25.83 mmol) of triethylamine in 80 mL of *N,N*-dimethylacetamide (DMA). The mixture was stirred for 16 h, followed by the addition of 500 mL of water. After filtration, the solid was washed using acetone, water, methanol, and ether, with a yield of 5.90 g, 79.9%. HRMS (FAB) m/z calcd for $C_{24}H_{17}N_2O_{10}$ ([M+H]⁺): 493.088; found: 493.088. Elemental analysis calcd for $C_{24}H_{16}N_2O_{10}$: C 58.54, H 3.28, N 5.69%; found: C 54.89, H 3.92, N 5.25%. ¹H NMR spectrum (300 MHz, DMSO-d_6, δ ppm) 13.4 (s, 4H, -COOH), 10.8 (s, 2H, -NH), 8.77 (s, 4H, Ar-H), 8.72 (s, 1H, Ar-H), 8.22 (d, 2H, Ar-H), 8.21 (d, 2H, Ar-H), 7.69 (t, 1H, Ar-H); ¹³C NMR spectrum (75 MHz, DMSO-d_6, δ ppm): 166.58, 165.34, 139.80, 134.70, 131.80, 131.17, 128.92, 127.23, 125.19, 124.76; IR spectrum (KBr, cm⁻¹): 3437 (br), 3394 (m), 3253 (br), 3160 (m), 3126 (m), 3092 (m), 2927 (m), 2856 (w), 2615 (br), 1712 (s), 1672 (s), 1611 (m), 1568 (s), 1489 (w), 1454 (m), 1430 (m), 1405 (m), 1338 (m), 1295 (m), 1285 (m), 1247 (m), 1217 (sh), 1150 (w), 1107 (w), 1085 (vw), 1001 (vw), 965 (vw), 951 (vw), 908 (w), 871 (vw), 818 (vw), 760 (m), 717 (w), 673 (m), 596 (w), 542 (vw), 490 (vw), 457 (vw).

Preparation of MOFs

Preparation of [Zn₂₈L¹₁₂(H₂O)₂₈](NO₃)₈·104DEF·30H₂O (PMOF-4). A solid mixture of 45 mg (0.099 mmol) of H₄L**1** and 148 mg (0.498 mmol) of Zn(NO₃)₂·6H₂O was dissolved in 5 mL of *N,N*-diethylformamide (DEF) in an 8 mL glass vial. The solution was heated in an oven at 85°C for 1–2 days, resulting in pale-yellow block crystals. The crystals were collected by filtration, washed with fresh DEF, and then air-dried. Yield: 133 mg, 83.6% (based on the ligand). Elemental analysis‡ calculated for [Zn₂₈L**1**₁₂(H₂O)₂₈](NO₃)₈·104DEF·30H₂O, (C₈₆₂H₁₃₈₀O₂₈₂N₁₁₂Zn₂₈): C 51.79, H 7.21, N 8.13%; found: C 51.50, H 7.21, N 8.51%. FT-IR (KBr, 4000–400 cm⁻¹): 3421 (br, w), 2978 (w), 2938 (w), 2878 (w), 1637 (vs), 1596 (m), 1578 (m), 1436 (m), 1384 (s), 1364 (s), 1302 (w), 1266 (w), 1214 (w), 1106 (w), 987 (w), 944 (w), 824 (w), 778 (w), 723 (w), 685 (w), 668 (w), 531 (w).

Preparation of [Zn₂₈L²₁₂(H₂O)₂₈](NO₃)₈·52DMA (PMOF-5). A solid mixture of 49 mg (0.099 mmol) of H₄L**2** and 148 mg (0.498 mmol) of Zn(NO₃)₂·6H₂O was dissolved in 2 mL DMA in a 5 mL glass vial. The solution sealed in a Pyrex tube was aged at 85°C for 5 days. The clear solution was cooled down to ambient temperature and stood for 3–4 days resulting in colorless octahedron-shaped crystals. The crystals were collected by filtration, washed with fresh DMA, and then air-dried. Yield: 43.5 mg, 39.9% (based on the ligand). Elemental analysis‡ calculated for [Zn₂₈L**2**₁₂(H₂O)₂₈](NO₃)₈·52DMA, (C₄₉₆H₆₆₈N₈₄O₂₂₄Zn₂₈): C 45.06, H 5.09, N 8.90%; found: H 4.95, C 45.25, N 8.88%. IR spectrum (KBr, 4000–400 cm⁻¹): 3421 (br, w), 3072 (w), 2936 (w), 2876 (w), 2794 (w), 1761 (w), 1720 (w), 1676 (w), 1616 (vs), 1556 (w), 1404 (w), 1385 (vs), 1264 (w), 1233 (w), 1195 (w), 1150 (w), 1103 (w), 1021 (w), 967 (w), 907 (w), 824 (w), 780 (w), 723 (w), 682 (w), 596 (w), 476 (w).

Crystallographic data collection and refinement of the structures. The diffraction data of PMOF-4 were measured using a single crystal coated with Paratone oil at 173 K with Mo Kα radiation on an X-ray diffraction camera system using a Bruker SMART CCD equipped with a graphite crystal incident beam monochromator. The SMART and SAINT software packages[19] were used for data collection and integration, respectively. The collected data were corrected for absorbance using SADABS,[20] based on Laue symmetry, using equivalent reflections. The diffraction data of PMOF-5 were measured using a single crystal coated with Paratone oil at 100 K with synchrotron radiation on an ADSC Quantum-210 detector at 2D SMC with a silicon (111) double crystal monochromator (DCM) at the Pohang Accelerator Laboratory, Korea. The ADSC Q210 ADX program[21] was used for data collection, and HKL3000[22] was used for cell refinement, reduction, and absorption correction. The crystal structures were solved by the direct method and were refined by full-matrix least-squares calculations using the SHELXTL program package.[23]

PMOF-4. [Zn₂₈L**1**₁₂(H₂O)₂₈](NO₃)₈ (C₃₁₂H₁₇₆N₈O₁₄₈Zn₂₈), fw = 8234.97 g·mol⁻¹, cubic, space group *Pm-3m*, a = b = c = 32.366(5) Å, V = 33906(8) Å³, Z = 1, μ (Mo Kα, λ = 0.71013 Å) = 0.509 mm⁻¹, 93319 reflections were collected, 3136 of which were unique [R_{int} = 0.4530]. Two zinc ions and two ligated water molecules at crystallographic 4*mm* symmetry sites (Wyckoff *f* site), the other two zinc ions and two ligated water molecules at crystallographic 3*m* symmetry sites (Wyckoff *g* site), and a ligand at a crystallographic *mm*2 symmetry site (Wyckoff *i* site) were

observed as an asymmetric unit. Counteranionic nitrate ions, which were probably disordered in the solvent pore, were not identified. All non-hydrogen atoms were refined anisotropically; the hydrogen atoms were assigned isotropic displacement coefficients U(H) = 1.2U (C) and their coordinates were allowed to ride on their respective atoms. The least-squares refinement of the structural model was performed under geometry restraints, such as DFIX, DANG, and FLAT, and displacement parameter restraints, such as ISOR, DEMU, and SIMU. The hydrogen atoms of the ligated water molecules were not included in the least-squares refinement. The final refinement was performed with the modification of the structure factors for the electron density of the disordered solvents (28365 $Å^3$, 83.7% of the total unit cell volume; 8581 solvent electrons correspond to eight nitrate anions and 149 DEF molecules per unit cell) using the SQUEEZE option of PLATON.[24] Refinement of the structure converged at a final $R1 = 0.2841$ and $wR2 = 0.5272$ for 2019 reflections with $I > 2\sigma(I)$; $R1 = 0.3461$ and $wR2 = 0.5560$ for all 3136 reflections. The largest difference peak and hole were 1.473 and -1.321 e·$Å^{-3}$, respectively.

PMOF-5. $[Zn_{28}L^2{}_{12}(H_2O)_{28}](NO_3)_8$ ($C_{288}H_{200}N_{32}O_{172}Zn_{28}$), fw = 8691.16 g·mol^{-1}, cubic, space group Pm-3, a = b = c = 31.102(4) Å, V = 30086(6) $Å^3$, Z = 1, μ (synchrotron, $\lambda = 1.00000$ Å) = 0.864 mm^{-1}, 18250 reflections were collected, 1748 of which were unique [R$_{int}$ = 0.0929]. Two zinc ions and two ligated water molecules at crystallographic $mm2$ symmetry sites (Wyckoff i site), the other two zinc ions and two ligated water molecules at crystallographic 3 symmetry sites (Wyckoff h site), and a ligand at a crystallographic m symmetry site (Wyckoff j site) were observed as an asymmetric unit. Counteranionic nitrate ions, which were probably disordered in the solvent pore, could not be identified. All non-hydrogen atoms were refined anisotropically; the hydrogen atoms were assigned isotropic displacement coefficients U(H) = 1.2U (C and N) and their coordinates were allowed to ride on their respective atoms. The least-squares refinement of the structural model was performed under geometry restraints, such as DFIX, DANG, and FLAT, and the displacement parameter restraint ISOR. The hydrogen atoms of the ligated water molecules were not included in the least-squares refinement. The final refinement was performed with the modification of the structure factors for the electron density of the disordered solvents (24176 $Å^3$, 80.4% of the total unit cell volume; 5275 solvent electrons correspond to eight nitrate anions and 105 DMA molecules per unit cell) using the SQUEEZE option of PLATON. Refinement converged at a final $R1 = 0.1101$ and $wR2 = 0.2660$ for 1134 reflections with $I > 2\sigma(I)$; $R1 = 0.1366$ and $wR2 = 0.2876$ for all 1748 reflections. The largest difference peak and hole were 0.343 and -0.247 e·$Å^{-3}$, respectively.

A summary of the crystal data and some crystallography data is given in Tables S1 and S2. CCDC 969629-30 contain the supplementary crystallographic data for PMOF-4 and PMOF-5. The data can be obtained free of charge at www.ccdc.cam.ac.uk/conts/retrieving.html or from the Cambridge Crystallographic Data Centre, 12 Union Road, Cambridge CB2 1EZ, UK.

Results and discussion

Preparation of the MOFs. The solvothermal reaction of $Zn(NO_3)_2$·$6H_2O$ with tetracarboxylic acid (H_4L^1 or H_4L^2) at an approximate 4–5:1 mole ratio under amide solvent (DEF or DMA) resulted in the MOF $[Zn_{28}L_{12}(H_2O)_{28}](NO_3)_8$·$xS$·$yH_2O$ (in which x and y are the number of solvent (DEF or DMA) molecules and water molecules, respectively; L = L^1 and S = DEF for PMOF-4; L = L^2 and S = DMA for PMOF-5) (Scheme 2).

$Zn(NO_3)_2$·$6H_2O$
+
H_4L
$\xrightarrow[\text{DEF or DMA}]{\text{at 85 °C}}$
$[Zn_{28}L_{12}(H_2O)_{28}](NO_3)_8$
PMOF-4: L = L^1
PMOF-5: L = L^2
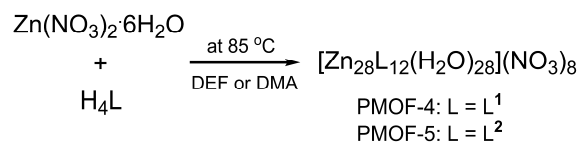
Scheme 2. Reaction Scheme.

Crystal structure of PMOF-4, $[Zn_{28}L^1{}_{12}(H_2O)_{28}](NO_3)_8$. The carboxylate residues of the ligand formed two different types of dinuclear Zn(II) clusters, $[Zn_2(COO)_4(H_2O)_2]$ and $[Zn_2(COO)_3(H_2O)_2]$, as SBUs in the network of PMOF-4. The $[Zn_2(COO)_4(H_2O)_2]$ SBU, which contained two 5-coordinate square-pyramidal Zn(II) centers, served as a 4-c node, and the $[Zn_2(COO)_3(H_2O)_2]$ SBU, which contained two tetrahedral Zn(II) centers, served as a 3-c node (Figure 1a and 1b). The 4-c $[Zn_2(COO)_4(H_2O)_2]$ SBUs at the six corners of the octahedron and the 3-c $[Zn_2(COO)_3(H_2O)_2]$ SBUs at the eight faces of the octahedron led to a 3,4-c rhombic dodecahedral MOP with 14 corners, 12 rhombic faces, and 28 edges as supramolecular TBU (Figure 1c). The outer diameter of the rhombic dodecahedral MOP was ~ 29 Å, and the diameter of the inner cavity was ~ 13 Å (Figure 2b). The rhombic dodecahedral MOPs were interconnected to each other via bent 1,3-phenylenedi-2,1-ethynediyl linkers of the ligands as a 24-c TBU node, but are quadruply interconnected to the six neighboring MOPs, to form a 3-D network with a **pcu** underlying topology based on the rhombic dodecahedral MOP as a topological 6-c octahedral node (Figure 2a). The quadruple linkage between the two MOPs generated a small cage-like pore (Figure 2c), and the primitive cubic linkage of the MOPs in the network with a **pcu** underlying topology led to a large cubic cavity with a diagonal dimension of ~ 23 Å (Figure 2d). The larger dimension of the rhombic dodecahedral MOP compared with that of the supercubic cavity did not allow the interpenetration of the network, which led to an extremely large solvent cavity in PMOF-4, corresponding to ~ 84% of the whole network structure. The $[Zn_2(COO)_4(H_2O)_2]$ SBU is neutral, whereas the $[Zn_2(COO)_3(H_2O)_2]$ SBU is mono cationic; hence, the framework is a cationic 3-D network. Although PMOF-4 must contain eight nitrate ions as counter anions per rhombic dodecahedral MOP unit, they could not be identified in the crystal structure because they were completely disordered in the solvent pore. An isoreticular MOF was reported using N-phenyl-N'-phenylbicyclo[2,2,2]oct-7-ene-2,3,5,6-tetracarboxdiimide tetracarboxylic acid as another tetracarboxylate ligand containing two 1,3-BDC units linked via a different bent covalent linker, in which the same rhombic dodecahedral MOPs were interconnected to the six neighboring MOPs to form a 3-D network with a **pcu** underlying topology.[25] However, the size of the supercubic cavity in this MOF was larger than that of the rhombic dodecahedral MOP, thus allowing the two-fold interpenetration of the network with a **pcu**

underlying topology.
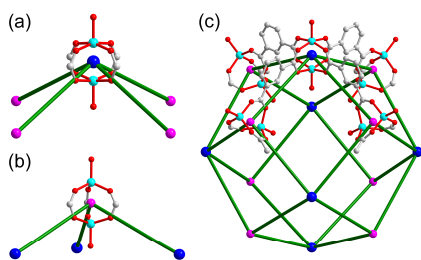
Figure 1. The SBUs and the TBU observed in PMOF-4. (a) A 4-c [Zn$_2$(COO)$_4$(H$_2$O)$_2$] square paddle-wheel SBU, (b) a 3-c [Zn$_2$(COO)$_3$(H$_2$O)$_2$] trigonal paddle-wheel SBU, and (c) a rhombic dodecahedral MOP made of six 4-c and eight 3-c SBUs as a TBU.
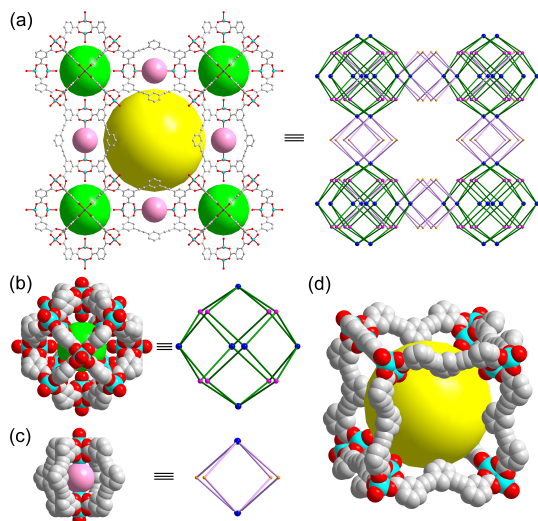
Figure 2. (a) Ball-and-stick and schematic packing diagrams of PMOF-4. Space-filling and schematic diagrams of (b) the cuboctahedral MOP as a TBU and (c) the quadruple linkage between the MOPs. (d) Supercubic cage generated via the primitive cubic packing arrangement of the cuboctahedral MOPs. The cavities in the centers of the MOP, the quadruple linkage, and the supercube are represented using green, pink, and yellow dummy balls.

Crystal structure of PMOF-5, [Zn$_{28}$L$^2_{12}$(H$_2$O)$_{28}$](NO$_3$)$_8$. PMOF-5 was also isoreticular to PMOF-4 (Figures S1 and S2). The 1,3-phenylenedi-2,1-ethynediyl linker residues containing rigid ethynyl linkages between the rhombic dodecahedral MOPs in PMOF-4 were replaced by the 1,3-phenylenebis(carbonylimino) residues containing flexible amide linkages in PMOF-5. Not only the 3,4-c rhombic dodecahedral MOP (Figure S1), but also the quadruple linkage between the MOPs in PMOF-4, were retained in PMOF-5, despite the increased flexibility of the L^2 ligand (Figures S2a and S2b). Although PMOF-5 was highly porous (the volume of the solvent cavity corresponded to ~ 80% of the total structure) and its underlying net topology was **pcu**, it was a noninterpenetrated network, as in PMOF-4, because the size of the rhombic dodecahedral TBU was larger than that of the supercubic cavity generated by the primitive cubic packing arrangement of the MOPs (Figure S2c).

Topology of the MOFs. In PMOF-4 and PMOF-5, the rhombic dodecahedral MOP could be considered as a 24-c rhombicuboctahedral TBU when the 24 branching edges of the rhombic dodecahedral MOP are considered as new 3-c nodes

(Figure 3a). It has been reported that the reactions of a Cu(II) ion with the same tetracarboxylate ligand and a similar tetracarboxylate ligand containing long bent organic linkers between the two 1,3-BDC residues may produce MOFs with the same underlying net topology, PMOF-3[16b] and [Cu$_{24}$(L)$_{12}$(H$_2$O)$_{16}$(DMSO)$_8$]$_n$ (in which L is 1,3-bis(5-methoxy-1,3-benzene dicarboxylate)benzene)[15a], both based on the same cuboctahedral MOP as a TBU. Among these MOFs, the cuboctahedral MOP could also be considered as a 24-c rhombicuboctahedral TBU when the 24 branching edges of the cuboctahedral MOP are considered as 3-c nodes (Figure 3b) and are quadruply interconnected to six neighboring MOPs, thus leading to a network with the same **pcu** underlying topology.[26,27]
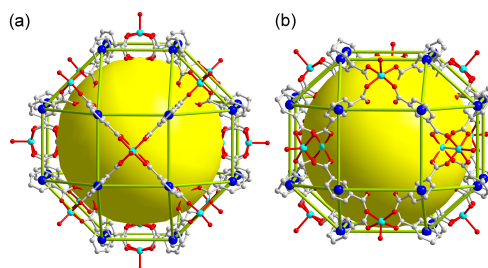
Figure 3. Rhombicuboctahedra based on (a) cuboctahedron and (b) rhombic dodecahedron.

Although the underlying topology of the isoreticular PMOF-4 and PMOF-5 is the same as that of PMOF-3 as a **pcu** topology, the complete net topology of the isoreticular PMOF-4 and PMOF-5 was different from that of PMOF-3. The net topology of PMOF-3 and [Cu$_{24}$(L)$_{12}$(H$_2$O)$_{16}$(DMSO)$_8$]$_n$ based on the [Cu$_2$(COO)$_4$] metal cluster as a 4-c SBU and the tetracarboxylate ligands as two linked 3-c nodes in different environments is a 3,3,4,4-c net with a **zmj** topology.[27,28] Conversely, the net topology of the isoreticular PMOF-4 and PMOF-5 based on the [Zn$_2$(COO)$_3$] and the [Zn$_2$(COO)$_4$] metal clusters as 3-c and 4-c nodes, respectively, and the tetracarboxylate ligand L^1 or L^2 as two linked 3-c nodes in the same environment was a 3,3,4-c net with a **zjz** topology (Figure 4).[28]
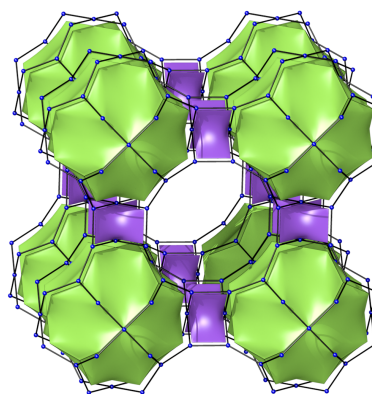
Figure 4. The net of **zjz** topology with green tiles representing the rhombic dodecahedral MOP as a TBU and purple tiles showing the **bb**-type linkage between the rhombic dodecahedral MOP units.

In the MOFs with a **zmj** topology, two different kinds of quadruple linkages, two **AA**-type linkages between the same two square faces of the cuboctahedral MOPs (Figures 5a and S3a), and four **BB**-type linkages between the same two square nodes of

the cuboctahedral MOPs (Figures 5b and S3b) were observed.[27] Interestingly, all the quadruple linkages in the isoreticular PMOF-4 and PMOF-5 based on the rhombic dodecahedral MOP are of the ***bb***-type of linkage between the two square nodes of the rhombic dodecahedral MOPs (Figures 5c and S3c), and were similar to the ***BB***-type linkage between the two square nodes of the cuboctahedral MOPs. This kind of quadruple linkage in the isoreticular PMOF-4 and PMOF-5 is also different to the ***AB***-type quadruple linkages between the square face of the cuboctahedral MOP and the square node of the cuboctahedral MOP (Figures 5d and S3d) in the other MOP-based MOF with a 3,3,3,3,4,4,4,4-c net with a **zhc** topology that is generated from the reaction of a Cu(II) ion with the ligand containing a short methylene linker between the two 1,3-BDC residues.[27,29]
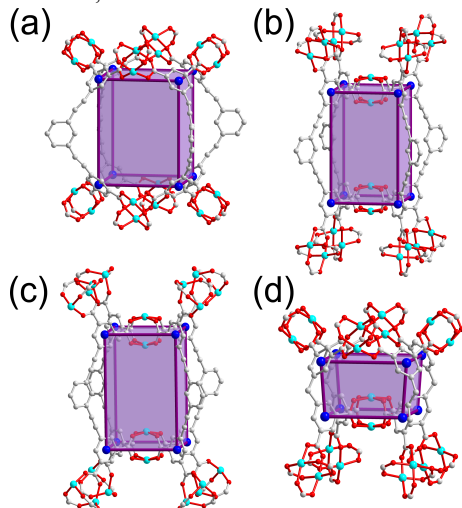

Figure 5. Four different types of quadruple linkages observed in the polyhedron-based MOFs with an underlying **pcu** topology. (a) ***AA***-type, (b) ***BB***-type, (c) ***bb***-type, and (d) ***AB***-type linkages.

The PXRD patterns of the as-synthesized samples were similar to the simulated patterns from the single crystal structures of PMOF-4 and PMOF-5, respectively (Figure 6). However, the MOFs at ambient condition lost their crystallinity (Figure S4). Although the MOFs have a large amount of solvent molecules at their potential pores (Figure S5), the removal of the solvent molecules from the pore via either a conventional vacuum-drying process or supercritical CO_2 activation process resulted in complete loss of crystallinity and the collapse of the porosity, leaving no significant N_2 sorption properties.
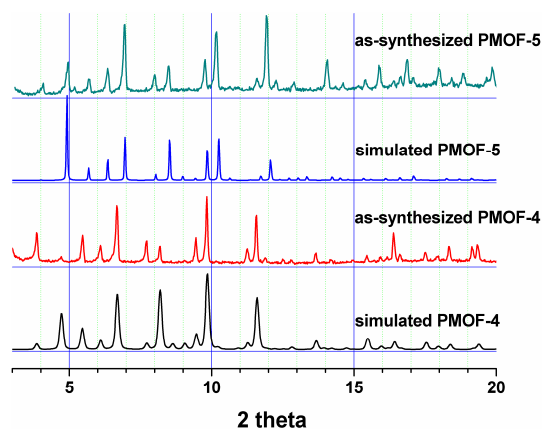
Figure 6. PXRD patterns of the as-synthesized samples of PMOF-4 and PMOF-5, which were ground under a small amount of mother liquor in an inert atmosphere.

Conclusions

The reactions of tetracarboxylate ligands containing two 1,3-BDC residues with a Cu(II) ion lead to MOFs based on the cuboctahedral MOP as a 24-c TBU because of the strong preference for the $[Cu_2(COO)_4]$ SBU. Conversely, similar reactions with the Zn(II) ion produced the two isoreticular MOP-based MOFs, PMOF-4 and PMOF-5, with a 3,3,4-c **zjz** topology, in which the MOP is a 3,4-c rhombic dodecahedron based on 3-c $[Zn_2(COO)_3]$ and 4-c $[Zn_2(COO)_4]$ SBUs. The MOP with 24 branching edges served as a 24-c rhombicuboctahedral TBU, which was quadruply linked to six neighboring rhombicuboctahedral TBUs in a **pcu** underlying topology. Although the underlying topology of PMOF-4 and PMOF-5 was the same as that of $[Cu_{24}(L)_{12}(H_2O)_{16}(DMSO)_8]_n$[15a] and PMOF-3[15b] with a 3,3,4,4-c **zmj** topology and of the PCN-12[28] of a 3,3,3,3,4,4,4,4-c **zhc** topology, the mode of the quadruple linkage in PMOF-4 and PMOF-5 is different from those in the other MOFs with different net topologies. In the MOFs of the net with a **zjz** topology, all the quadruple linkages are of the same ***bb***-type, where the four edges that are directly involved in the formation of the $Zn_2(COO)_4$ SBU are interlinked to the same types of the four edges directly involved in the formation of the $Zn_2(COO)_4$ SBU.

The difference in the net topology of the Zn-based MOF and those of the reported Cu-based MOFs stems from the different preference for the SBUs. While a Cu(II) ion with a ligand containing carboxylate residue exhibited a strong preference for the square-paddle-wheel $[Cu_2(COO)_4]$ SBU, a Zn(II) ion could adopt not only the square-paddle-wheel $[Zn_2(COO)_4]$ cluster as a 4-c SBU, but also the trigonal-paddle-wheel $[Zn_2(COO)_3]$ cluster as a 3-c SBU.

Notes and references

[a]*Department of Chemistry, Ulsan National Institute of Science & Technology, Ulsan, 689-798, Korea. Fax: 82 52 217 2019; Tel: 82 52 217 2931; E-mail: mslah@unist.ac.kr*
[b]*Current address: Changzhou Exit-Entry Inspection and Quarantine Bureau*
[c]*Department of Chemistry, Zhejiang Sci-Tech University, Hangzhou, 310018, China. E-mail: zouyang@zstu.edu.cn*
[d]*Department of Chemistry, Pohang University of Science and Technology, Pohang 790-784, Korea.*

† Electronic Supplementary Information (ESI) available: tables of crystal data and structure refinements, ball-and-stick and space-filling drawings of the crystal structure of PMOF-5, quadruple linkages between the MOPs, PXRD data, TGA data, and crystallographic information files in CIF format. See DOI: 10.1039/b000000x/

‡ The extent to which the solvent molecules occupy the cavity varies depending on exposure time of the sample in air. After several days, the elemental analysis of an air-dried sample was carried out.

1. M. G. Goesten, F. Kapteijn and J. Gascon, *CrystEngComm*, 2013, **15**, 9249-9257.
2. Y. Zhu, P. Yin, F. Xiao, D. Li, E. Bitterlich, Z. Xiao, J. Zhang, J. Hao, T. Liu, Y. Wang and Y. Wei, *J. Am. Chem. Soc.*, 2013, **135**, 17155-17160.

CrystEngComm Accepted Manuscript

3. (a) S. S.-Y. Chui, S. M.-F. Lo, J. P. H. Charmant, A. G. Orpen and I. D. Williams, *Science*, 1999, **283**, 1148-1150; (b) J. L. C. Rowsell and O. M. Yaghi, *J. Am. Chem. Soc.*, 2006, **128**, 1304-1315; (c) S. Xiang, W. Zhou, J. M. Gallegos, Y. Liu and B. Chen, *J. Am. Chem. Soc.*, 2009, **131**, 12415-12419; (d) P. Chowdhury, C. Bikkina, D. Meister, F. Dreisbach and S. Gumma, *Micropor. Mesopor. Mater.*, 2009, **117**, 406-413.

4. O. Delgado-Friedrichs, M. O'Keeffe and O. M. Yaghi, *Acta Cryst.*, 2006, **A62**, 350-355.

5. S. A. Bourne, J. Lu, A. Mondal, B. Moulton and M. J. Zaworotko, *Angew. Chem. Int. Ed.*, 2001, **40**, 2111-2113.

6. (a) M. Eddaoudi, J. Kim, J. B. Wachter, H. K. Chae, M. O'keeffe and O. M. Yaghi, *J. Am. Chem. Soc.*, 2001, **123**, 4368-4369; (b) B. Moulton, J. Lu, A. Mondal and M. J. Zaworotko, *Chem. Commun.*, 2001, 863-864.

7. (a) B. Singh, J. R. Long, F. Fabrizi de Biani, D. Gatteschi and P. Stavropoulos, *J. Am. Chem. Soc.*, 1997, **119**, 7030-7047; (b) O. R. Evans, R. G. Xiong, Z. Wang, G. K. Wong and W. Lin, *Angew. Chem. Int. Ed.*, 1999, **38**, 536-538; (c) J. C. Noveron, M. S. Lah, R. E. Del Sesto, A. M. Arif, J. S. Miller and P. J. Stang, *J. Am. Chem. Soc.*, 2002, **124**, 6613-6625; (d) D. J. Darensbourg, J. R. Wildeson and J. C. Yarbrough, *Inorg. Chem.*, 2002, **41**, 973-980; (e) J. Rabone, Y.-F. Yue, S. Y. Chong, K. C. Stylianou, J. Bacsa, D. Bradshaw, G. R. Darling, N. G. Berry, Y. Z. Khimyak, A. Y. Ganin, P. Wiper, C. J. B. and M. J. Rosseinsky, *Science*, 2010, **329**, 1053-1057; (f) Z.-H. Zhang, S.-C. Chen, J.-L. Mi, M.-Y. He, Q. Chen and M. Du, *Chem. Commun.*, 2010, **46**, 8427-8429.

8. (a) H. Li, M. Eddaoudi, M. O'Keeffe and O. M. Yaghi, *Nature*, 1999, **402**, 276-279; (b) H. K. Chae, D. Y. Siberio-Pérez, J. Kim, Y. Go, M. Eddaoudi, A. J. Matzger, M. O'Keeffe and O. M. Yaghi, *Nature*, 2004, **427**, 523-527; (c) M. Eddaoudi, N. Rosi, D. Vodak, J. B. Wachter, M. O'Keeffe and O. M. Yaghi, *Science*, 2002, **295**, 469-472; (d) H. K. Chae, J. Kim, O. Delgado-Friedrichs, M. O'Keeffe and O. M. Yaghi, *Angew. Chem. Int. Ed.*, 2003, **42**, 3907-3909; (e) L. Rajput, S. Hong, X. Liu, M. Oh, D. Kim and M. S. Lah, *CrystEngComm*, 2011, **13**, 6926-6929.

9. (a) H. Li, C. E. Davis, T. L. Groy, D. G. Kelley and O. M. Yaghi, *J. Am. Chem. Soc.*, 1998, **120**, 2186-2187; (b) C. A. Williams, A. J. Blake, P. Hubberstey and M. Schröder, *Chem. Commun.*, 2005, 5435-5437; (c) J. Y. Lee, L. Pan, S. P. Kelly, J. Jagiello, T. J. Emge and J. Li, *Adv. Mater.*, 2005, **17**, 2703-2706; (d) S. J. Garibay, J. R. Stork, Z. Wang, S. M. Cohen and S. G. Telfer, *Chem. Commun.*, 2007, 4881-4883.

10. (a) H. Li, M. Eddaoudi, T. L. Groy and O. M. Yaghi, *J. Am. Chem. Soc.*, 1998, **120**, 8571-8572; (b) D. N. Dybtsev, H. Chun and K. Kim, *Angew. Chem. Int. Ed.*, 2004, **43**, 5033-5036; (c) H. Chun, *J. Am. Chem. Soc.*, 2008, **130**, 800-801.

11. (a) J. Lu, A. Mondal, B. Moulton and M. J. Zaworotko, *Angew. Chem. Int. Ed.*, 2001, **40**, 2113–2116; (b) M. Wu, F. Jiang, W. Wei, Q. Gao, Y. Huang, L. Chen and M. Hong, *Cryst. Growth Des.*, 2009, **9**, 2559-2561; (c) T.-F. Liu, J. Lü, Z. Guo, D. M. Proserpio and R. Cao, *Cryst. Growth Des.*, 2010, **10**, 1489-1491; (d) X. Zhao, H. He, F. Dai, D. Sun and Y. Ke, *Inorg. Chem.*, 2010, **49**, 8650-8652.

12. (a) J. I. Feldblyum, M. Liu, D. W. Gidley and A. J. Matzger, *J. Am. Chem. Soc.*, 2011, **133**, 18257-18263; (b) X. Song, S. Jeong, D. Kima and M. S. Lah, *CrystEngComm*, 2012, **14**, 5753-5756; (c) M. K. Bhunia, J. T. Hughes, J. C. Fettinger and A. Navrotsky, *Langmuir*, 2013, **29**, 8140-8145.

13. (a) O. M. Yaghi, C. E. Davis, G. Li and H. Li, *J. Am. Chem. Soc.*, 1997, **119**, 2861-2868; (b) M. Eddaoudi, H. Li and O. M. Yaghi, *J. Am. Chem. Soc.*, 2000, **122**, 1391-1397; (c) X.-R. Hao, X.-L. Wang, K.-Z. Shao, G.-S. Yang, Z.-M. Su and G. Yuan, *CrystEngComm*, 2012, **14**, 5596-5603; (d) M. Oh, L. Rajput, D. Kim, D. Moon and M. S. Lah, *Inorg. Chem.*, 2013, **52**, 3891-3899.

14. O. Delgado-Friedrichs, M. O'Keeffe and O. M. Yaghi, *Acta Cryst.*, 2002, **A59**, 22-27.

15. (a) H. Furukawa, J. Kim, N. W. Ockwig, M. O'Keeffe and O. M. Yaghi, *J. Am. Chem. Soc.*, 2008, **130**, 11650-11661; (b) J.-R. Li and H.-C. Zhou, *Nature Chem.*, 2010, **2**, 893-898; (c) L.-B. Sun, J.-R. Li, W. Lu, Z.-Y. Gu, Z. Luo and H.-C. Zhou, *J. Am. Chem. Soc.*, 2012,

134, 15923-15928; (d) W. Wei, W. Li, X. Wang and J. He, *Cryst. Growth Des.*, 2013, **13**, 3843-3846.

16. (a) J. J. Perry IV, V. C. Kravtsov, G. J. McManus and M. J. Zaworotko, *J. Am. Chem. Soc.*, 2007, **129**, 10076-10077; (b) X. Liu, M. Park, S. Hong, M. Oh, J. W. Yoon, J.-S. Chang and M. S. Lah, *Inorg. Chem.*, 2009, **48**, 11507-11509; (c) X. S. Wang, Ma, P. M. Forster, D. Yuan, J. Eckert, J. J. López, B. J. Murphy, J. B. Parise and H. C. Zhou, *Angew. Chem. Int. Ed.*, 2008, **47**, 7263-7266; (d) G. J. McManus, Z. Wang and M. J. Zaworotko, *Cryst. Growth Des.*, 2004, **4**, 11-13; (e) D. Yuan, D. Zhao, D. Sun and H. C. Zhou, *Angew. Chem. Int. Ed.*, 2010, **49**, 5357-5361; (f) B. Zheng, J. Bai, J. Duan, L. Wojtas and M. J. Zaworotko, *J. Am. Chem. Soc.*, 2010, **133**, 748-751; (g) B. Li, Z.-H. Zhang, Y. Li, K. Yao, Y. Zhu, Z. Deng, F. Yang, X. Zhou, G. Li, H. Wu, N. Nijem, Y. J. Chabal, Z. Lai, Y. Han, Z. Shi, S. Feng and J. Li, *Angew. Chem. Int. Ed.*, 2012, **51**, 1412-1415; (h) O. K. Farha, I. Eryazici, N. C. Jeong, B. G. Hauser, C. E. Wilmer, A. A. Sarjeant, R. Q. Snurr, S. T. Nguyen, A. O. Yazaydın and T. Hupp, *J. Am. Chem. Soc.*, 2012, **134**, 15016-15021; (i) Y. Yan, M. Suyetin, E. Bichoutskaia, A. J. Blake, D. R. Allan, S. A. Barnett and M. Schröder, *Chem. Sci.*, 2013, **4**, 1731-1736.

17. (a) Y. Zou, M. Park, S. Hong and M. S. Lah, *Chem. Commun.*, 2008, 2340-2342; (b) S. Hong, M. Oh, M. Park, J. W. Yoon, J.-S. Chang and M. S. Lah, *Chem. Commun.*, 2009, 5397-5399; (c) L. Li, S. Tang, X. Lv, M. Jiang, C. Wang and X. Zhao, *New J. Chem.*, 2013, **37**, 3662-3670.

18. *Materials Studio*, version 4.3; Accelrys: San Diego, CA, 2008.

19. SMART and SAINT, *Area Detector Software Package and SAX Area Detector Integration Program*; Bruker Analytical X-Ray; Madison, WI, USA, 1997.

20. SADABS, *Area Detector Absorption Correction Program*; Bruker Analytical X-Ray; Madison, WI, USA, 1997

21. A. J. Arvai and C. Nielsen, *ADSC Quantum-210 ADX Program*, Area Detector System Corporation; Poway, CA, USA, 1983.

22. HKL3000: Z. Otwinowski and W. Minor; in Methods in Enzymology, ed. C. W. Carter, Jr. and R. M. Sweet, Academic Press, New York, 1997, vol. 276, part A, pp. 307.

23. SHELX program: G. M. Sheldrick, *Acta Cryst.*, 2008, **A64**, 112.

24. PLATON program: A. L. Spek, *Acta Cryst.*, **D65**, 2009, 148-155.

25. Z.-J. Zhang, W. Shi, Z. Niu, H.-H. Li, B. Zhao, P. Cheng, D.-Z. Liao and S.-P. Yan, *Chem. Commun.*, 2011, **47**, 6425-2427.

26. J. J. Perry Iv, J. A. Perman and M. J. Zaworotko, *Chem. Soc. Rev.*, 2009, **38**, 1400-1417.

27. M. O'Keeffe and O. M. Yaghi, *Chem. Rev.*, 2012, **112**, 675-702.

28. V. A. Blatov, *IUCr CompComm Newsletter*, 2006, 7, 4-38, TOPOS is available at http://www.topos.ssu.samara.ru/.

29. X.-S. Wang, S. Ma, P. M. Forster, D. Yuan, J. Eckert, J. J. López, B. J. Murphy, J. B. Parise and H.-C. Zhou, *Angew. Chem. Int. Ed.*, 2008, **47**, 7263–7266.

CrystEngComm Accepted Manuscript

Graphic content:

The solvothermal reactions of a Zn(II) ion with ligands containing two 1,3-benzene dicarboxylate residues resulted in isoreticular MOFs with a 3,3,4-c **zjz** topology based on a rhombic dodecahedral metal–organic polyhedron (MOP), in which the rhombic dodecahedral MOP was built using six $[Zn_2(COO)_4]$ clusters as a 4-c SBU and eight $[Zn_2(COO)_3]$ clusters as a 3-c SBU.

$[Zn_{28}L_{12}(H_2O)_{28}](NO_3)_8$